Available online at www.sciencedirect.com
ScienceDirect
Chemical Physics 330 (2006) 394–400
Chemical Physics
www.elsevier.com/locate/chemphys

Kinetics and mechanism of 2-pyridylacetic acid pyrolysis in the gas phase: A joint experimental and theoretical study

M. Izadyar [a,*], N. Zamani [b], M.R. Gholami [c]

[a] Department of Chemistry, University of Payam-e-Noor, P.O. Box 43, Khorasan-e-Razavi, Gonabad, Iran
[b] Education organization of Khorasan-e-Razavi, Education management of Gonabad, Gonabad, Iran
[c] Department of chemistry, Sharif University of Technology, Tehran, Iran

Received 30 August 2005; accepted 11 September 2006
Available online 19 September 2006

Abstract

A combination of the experimental and theoretical study was carried out on the reaction mechanism associated with the pyrolysis of 2-pyridylacetic acid in the gas phase. Methylpyridine and carbon dioxide were analyzed as the products, using a static system over the pressure range of 18–55 torr and the temperature of 541.2–583.4 K. The experimental kinetic data show that the pyrolysis process is homogeneous, unimolecular and proceeds through a concerted mechanism. Theoretical studies at the B3LYP level using the 6-31G* basis set confirmed an asynchronous concerted mechanism for the reaction. Computed kinetic and activation parameters are in good agreement with the experimental one.

Keywords: 2-Pyridylacetic acid; Asynchronous concerted mechanism; Homogeneous; Pyrolysis; Gas phase kinetic; Unimolecular reaction

1. Introduction

Recent studies on the gas phase pyrolysis reactions of 2-substituted chloro, hydroxyl, alkoxy, phenoxy and acetoxy carboxylic acids [1–5] show that the acidic H of the COOH group assists as the leaving group for the elimination. Through these reactions the unstable α-lacton (Scheme 1) has been formed. The α-lactone decomposes rapidly, yielding carbon monoxide and the corresponding carbonyl compound.

If an amino or nitrogen derivative is considered as a leaving group L in organic compounds, it will be difficult for the pyrolysis reaction to proceed through the Scheme 1. Therefore, gas phase pyrolysis for some kinds of amino acids which undergo a different mechanism may be described as Scheme 2.

Some reports on the pyrolysis of amino acids and their sodium salts explain that the experimental techniques are inadequate to determine all of the products and these processes occurred in different manner [6–8]. Also, the experimental and theoretical studies on the several amino acids confirmed that the corresponding zwitterions compounds cannot be produced in the gas phase [9].

In view of the scare information on the gas phase pyrolysis of amino acids including the theoretical and mechanistic consideration, a combined experimental and theoretical study aimed at investigation of 2-pyridylacetic acid pyrolysis in the gas phase.

2. Experimental

2-Pyridylacetic acid hydrochloride was purchased from Aldrich. The hydrochloride was converted to free acids by treatment with fresh Ag_2CO_3, filtration of the resultant AgCl precipitate, precipitation of dissolved Ag with H_2S and evaporation to dryness.

Cyclohexene was synthesized according to literature [10] to be applied as a free radical inhibitor in the gas phase.

* Corresponding author. Tel.: +98 5357259200; fax: +98 5357259204.
E-mail address: Izadyar.m@gmail.com (M. Izadyar).

0301-0104/$ - see front matter © 2006 Elsevier B.V. All rights reserved.
doi:10.1016/j.chemphys.2006.09.010

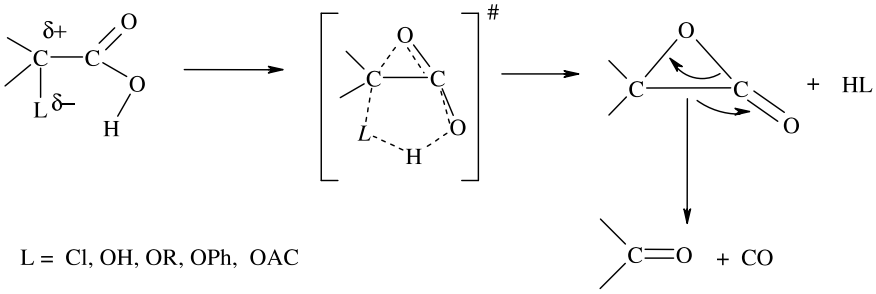

Scheme 1.

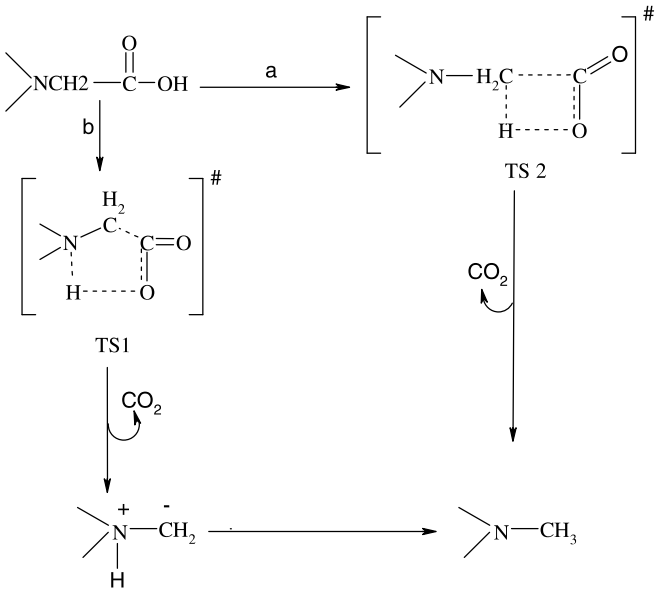

Scheme 2.

The products structures were confirmed by the gas chromatography mass spectroscopy using a HP-5793 instrument fitted with a 30 m × 0.25 mm i.d. and HP-5 capillary column.

The pyrolysis experiments were performed in a static system over 10 half-lives in the presence of the free radical scavenger (cyclohexene).

2-Pyridyl acetic acid (2PAA) was dissolved in glacial acetic acid and injected directly into the reaction vessel (~20 μL), using a microsyring (HP, Agilent 5181-1267). The reaction mixture was injected into the GC instrument (HP, Agilent serie 6890), equipped with a thermal conductivity detector (TCD) in each kinetic run.

Gaseous mixture at the definite interval times by a gastight syringe (PS, A-2) was injected into the GC capillary column (HP-5, 30 m × 0.32 mm i.d.). The experimental techniques have been described elsewhere [11].

3. Computational details

The structures corresponding to the reactant, intermediate, transition state and the products for the pyrolysis reaction were optimized, using the Gaussian 98 computational package [12] with the DFT method as implemented in the computational program.

Since, in addition to the results of our previous studies [11,13–17], Lee and co-workers have previously reported that the B3LYP hybrid functional gives structures and vibrational frequencies in less time rather than other theoretical methods which are in good agreement with the coupled-cluster theory [18], the optimized geometries of the stationary points on the potential energy surface (PES) were obtained using the Becke's three parameter hybrid exchanges functional with the correlation functional of Lee, Yang and Parr (B3LYP) level of the theory with the 6-31 G* basis set.

The synchronous transit-guided quasi-Newton (STQN) method as implemented by Schlegel et al. was used to locate the TS [19].

Vibrational frequencies for the points along the reaction paths were determined to provide an estimation of the zero point vibrational energies (ZPVE).

Activation parameters were calculated in the temperature range of the pyrolysis reaction at the B3LYP level of the theory with the different basis sets. Activation energy, E_a, and the Arrhenious factor were computed using the Eqs. (1) and (2), respectively. These equations have been derived from the transition state theory [20,21]:

$$E_a = \Delta H^{\neq}(T) + RT \quad (1)$$

$$A = (eK_B T/h)\exp(\Delta S^{\neq}(T)/R) \quad (2)$$

Thermodynamic parameters for the global reaction were calculated at 298.15 K. Also charge changes on the atoms for the reactant, TS, intermediate and methyl pyridine and bond orders through the pyrolysis reaction have been computed by means of the natural bond orbital (NBO) analysis [22,23].

4. Results and discussion

4.1. Experimental results

According to Scheme 3, pyrolysis reaction of 2PAA demands $P_f/P_0 = 2.0$, where P_f and P_0 are the final to initial pressures, respectively. The average experimental P_f/P_0 value at five different temperatures between 541.2 K and

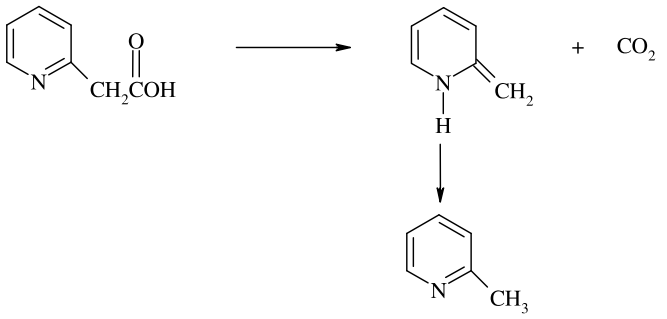

Scheme 3.

Table 1
Ratio of final to initial pressure in the gas phase

T (K)	P_0	P_f	P_f/P_0	Average
541.2	31.2	61.78	1.98	
550.5	38.7	66.56	1.72	
561.3	42.6	74.12	1.74	
572.6	49.1	99.12	2.02	
583.4	55.4	101.38	1.83	1.87

583.4 K and 10 half-lives is 1.87 (Table 1). Additional confirmation of the stoichiometry up to 82% pyrolysis was obtained with comparing the pressure measurements using the quantitative analysis of carbon dioxide formation (Table 2).

The homogeneity of this process was studied using the vessels with a surface-to-volume ratio of 3.0 and 6.0 times greater than the unpacked vessel. No important differences in the rate coefficients were obtained. This indicates that the pyrolysis reaction is homogeneous (Table 3).

The effect of different proportions of cyclohexene is shown in Table 4 which indicates that the reaction is molecular and not free radical in nature.

Table 2
Stoichiometry of the reaction in the gas phase

Time (s)	30	100	200	400	700
Reaction (% pressure)	19.5	40.8	66.2	81.8	92.7
CO_2 (% chromatography)	20.1	41.2	67.7	80.3	93.4

Table 3
Homogeneity of the pyrolysis reaction in the gas phase at 541.2 K

S/V (cm^{-1})	10^4k (S^{-1})	% Difference
1.0	1.44	0.00
3.0	1.49	3.59
6.0	1.38	4.61

Table 4
Effects of cyclohexene on the rate coefficients at 572.6 K

P_i/P_{2PAA}	10^4k (S^{-1})	% Difference
0	9.30	0.00
1	9.47	1.83
2	9.11	−2.04

The first-order rate coefficients for the reaction calculated from $k = (2.303/t)\log[P_0/(2P_0 - P_t)]$ were found to be independent of the initial pressure (Table 5). The average k value is estimated within ±5% standard deviation. A good straight line up to 82% decomposition was achieved by means of plotting the $\log(2P_0 - P_t)$ versus time t (Fig. 1). The variations of the first order rate coefficient with the temperature are given in Table 6. A least square fit of the rate coefficients in the form of the Arrhenious equation produced the following relationship:

$$\log k = (10.90 \pm 0.32) - (152.74 \pm 2.02\ \mathrm{kJ\,mol^{-1}})(2.303RT)^{-1}$$
$$R = 8.314\ \mathrm{J\,mol^{-1}\,K^{-1}}$$

Activation parameter values for 2PAA are listed in Table 7. Activation energy for the pyrolysis reaction of 2PAA is nearly small relative to similar amino acids such

Table 5
Variation of the rate coefficients with the initial pressure at 541.2 K

P_0 (Torr)	18	25	37	50
10^4k (S^{-1})	1.44	1.47	1.39	1.50

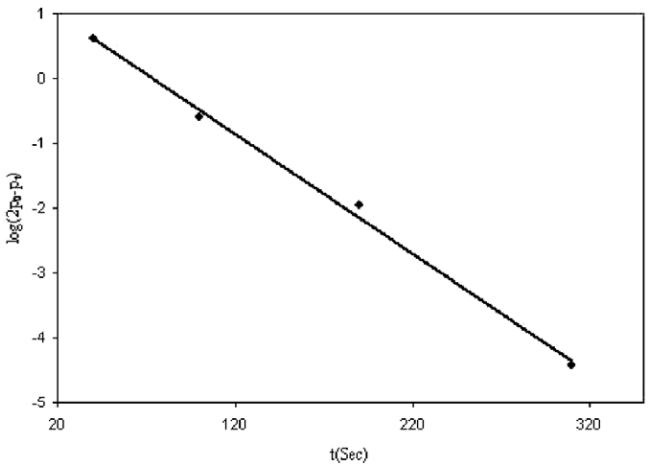

Fig. 1. Plot of $\log(2P_0 - P_t)$ versus time at 561.3 K.

Table 6
Variation of the rate coefficients with the temperature in the gas phase

T (K)	10^4k (S^{-1})	$-\ln k$	σ (%)
541.2	1.44	8.85	1.53
550.5	2.57	8.27	4.39
561.3	4.87	7.63	3.92
572.6	9.30	6.98	4.81
583.4	16.84	6.39	4.13

Table 7
Experimental kinetic and activation parameters for the pyrolysis reaction in the gas phase

Ea (kJ mol^{-1})	$\log A$	$\Delta H^{\neq}$ (kJ mol^{-1})	$\Delta G^{\neq}$(kJ mol^{-1})	$-\Delta S^{\neq}$ (J mol^{-1} K^{-1})
152.74	10.90	148.07	176.06	49.82

as picolinic acid [24]. This small difference may be attributed to the facile formation of six-center TS for 2PAA rather than five-member TS for picolinic acid. The concerted nature of the reaction could be confirmed by negative values for the activation entropy, too.

4.2. Theoretical results

Three possible mechanisms can be suggested for the pyrolysis of 2PAA in the gas phase. The first one may be started by the homogeneous cleavage of C4–C5 bond according to Scheme 4, follows by a step-wise radical mechanism. The second possibility is the proceeding through a zwitterionic state in Scheme 5 and the third is direct unimolecular splitting through a concerted mechanism.

C4–C5 bond breaking is the rate determining step in the first mechanism. The C4–C5 bond dissociation energy would be the activation energy of the reaction from the energy point of view.

After full geometry optimization of the probable radicals, their energies were calculated with the UB3LYP level of the theory using a variety of different basis sets. Including the different polarization and diffusion effects. It is obvious from the Table 8 that the calculated activation energies are much greater than the experimental one; therefore the step-wise mechanism is unacceptable.

According to the experimental value for activation entropy, the zwitterionic mechanism can not be reasonable in the gas phase. These conclusions led us to the last mechanism and concerted mechanism was fully investigated.

The concerted pathway involves a two-step mechanism. The first step which is initiated with the H1–N2 bond formation and C4–C5 bond cleavage is a concerted process in which an cyclic intermediate and carbon dioxide are formed via a six-membered cyclic TS (TS1) according to Fig. 2, where the hydrogen atom of the OH of the carboxyl group migrates to the nitrogen atom of the pyridine ring. The second step is a rapid process in which the aromaticity of the ring is conserved by the hydrogen atom transfer through a four-membered cyclic TS (TS2). Carbon dioxide and methyl pyridine (Prod1) are the major products of the first and second step, respectively.

During the pyrolysis process, when the reactant is transformed to the TS1, H1–N2, C5–O6 and C3–C4 bond lengths decrease, whereas H1–O6, N2–C3 and C4–C5 bond

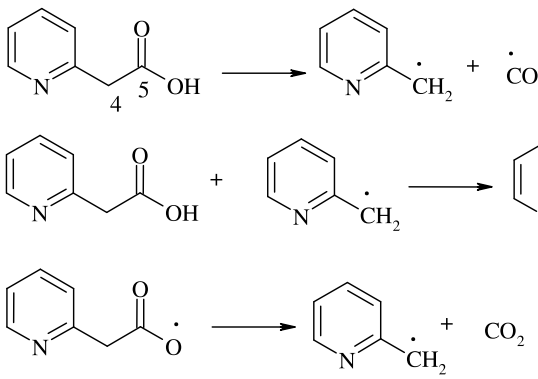

Scheme 4.

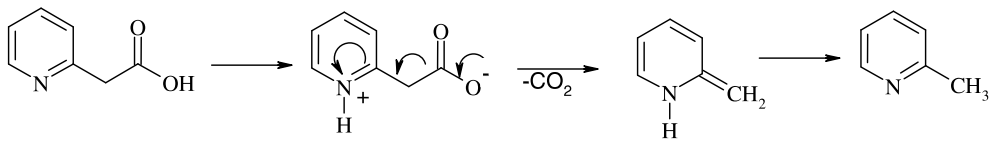

Scheme 5.

Table 8
Calculated energies (Hartree) using the UB3LYP method (Py = C5H4N)

Basis set	·COOH	Py–CH_2COO·	Py–C·H_2	2PAA	CO_2	$\Delta E^{\neq}$ (kJ mol^{-1})
6-31G*	189.0878	475.4909	286.9289	476.1729	188.5809	410.08
6-31 + G*	189.1005	475.5118	286.9419	476.1945	188.5903	399.52
6-31 + G**	189.1062	475.5208	286.9511	476.2091	188.5904	398.48
6-311G*	189.1447	475.6038	286.9902	476.2873	188.6408	400.24
6-311 + G*	189.1518	475.6153	286.9953	476.2983	188.6466	397.11
6-311 + G**	189.1586	475.6249	287.0054	476.3147	188.6466	395.60

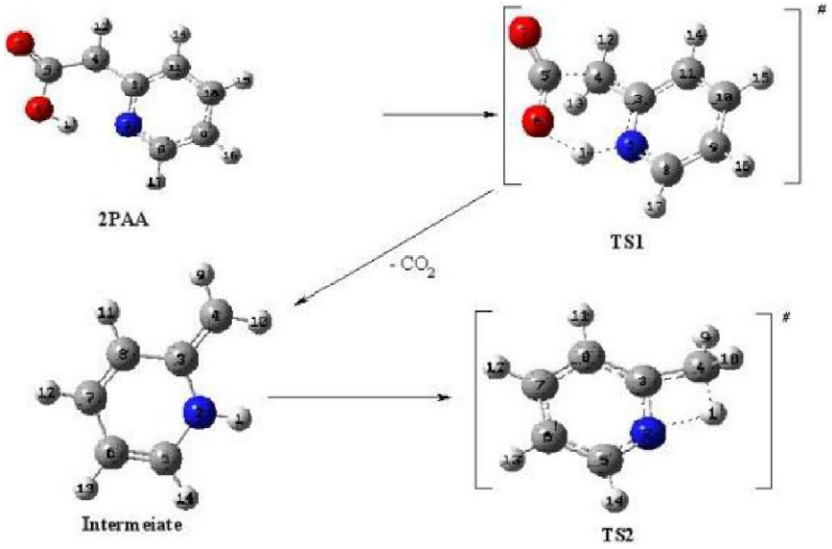

Fig. 2. Suggested concerted mechanism for the pyrolysis of 2PAA in the gas phase.

lengths increase. Table 9 shows the geometric parameters for the reactant, TS and intermediate according to atom numbering on Fig. 2. The comparison between the H1–N2 and C4–C5 bond lengths at the TS1 with the same one in the reactant indicates that the H1–N2 bond formation occurs faster than C4–C5 bond cleavage. Accordingly the new bond formation happens by a slightly asynchronous nature for the concerted mechanism. In Table 9 we can notice that the C–C bond lengths of the ring change from the reactant to the products which confirm that the ring aromaticity fluctuates through the reaction.

Charge distribution on the reactant and the TS1 was calculated using the NBO analysis. It can be concluded from Table 10 that a large positive charge develops on H1 atom, while N2 atom supports the electronic excess in the reactant. The negative character of N2 atom allows it to attract the positive character of H1 atom at the TS1, which confirms the cyclic TS1. On the other hand the electron density increases for H1 atom and decreases for C5 atom (positive character of C5 and negative one for H1 atom) at the TS1 showing that the new bond formation of H1–N2 is faster than C4–C5 bond cleavage which confirms an asynchronous nature for the concerted mechanism.

High magnitudes of the imaginary vibrational frequencies for the TS1 (>1000 icm^{-1} in all of the theoretical levels) indicate that this point is associated with the light atom movement of H1 at the TS1.

Dipole moment changes through the pyrolysis reaction justify the greater polarity of the reactant relative to the TS1. Considering the decrease of dipole moments through the reaction, one can confirm that charge symmetry decreases for the TS1 in comparison to the reactant. This could be another reason for the concerted nature of the reaction mechanism.

Calculated kinetic and thermodynamic parameters for the pyrolysis reaction at 561 and 298 K, respectively, are reported in Table 11. It can be concluded from Table 11

Table 9
Optimized geometric parameters (bond lengths in angstrom, angles in degree) for the reactants (2PAA), intermediate (Int) and transition state (TS) using the B3LYP/6-31G* method in the gas phase

Parameter	2PAA	TS1	Int
H1–N2	1.80	1.26	1.01
N2–C3	1.34	1.38	1.40
C3–C4	1.51	1.38	1.35
C4–C5	1.54	1.80	–
C5–O6	1.33	1.30	–
C5–O7	1.20	1.19	–
N2–C8	1.33	1.36	1.40
C8–C9	1.39	1.36	1.34
C9–C10	1.39	1.42	1.43
C10–C11	1.39	1.37	1.35
C11–C3	1.39	1.43	1.45
H1–O6–C5	41.66	106.15	–
C4–C5–O6	116.03	110.04	–
N2–C3–C4	116.57	118.92	121.17
N2–C3–C4–C5	45.65	56.06	–

Table 10
Calculated NBO charges for the reactant (2PAA), TS, intermediate (Int) and Methyl pyridine (Prod 1) in the gas phase using the B3LYP/6-31G* method

Atom	2PAA	TS1	Int	Prod 1
H1	0.51	0.48	0.42	0.24
N2	−0.52	−0.54	−0.58	−0.46
C3	0.23	0.24	0.12	0.22
C4	−0.61	−0.63	−0.57	−0.70
C5	0.83	0.87	–	–
O6	−0.72	−0.72	–	–
O7	−0.58	−0.58	–	–
C8	0.05	0.05	0.03	0.05
C9	−0.28	−0.29	−0.35	−0.29
C10	−0.18	−0.18	−0.22	−0.20
C11	−0.26	−0.25	−0.24	−0.27

Table 11
Calculated gas phase relative (activation) energies (in kJ mol^{-1}, E = Total energy, H = Enthalpy, G = Gibbs free energy) for the structures involved in the pyrolysis reaction at the B3LYP level (T = 561.8 K)

Structure	Basis set	ΔE	ΔH	ΔG
2PAA	6-31G*	0.0	0.0	0.0
Int + CO_2	6-31G*	70.9	66.2	−23.5
Prod 1 + CO_2	6-31G*	−46.0	−48.5	−97.8
TS2	6-31G*	131.5	129.0	46.3
	6-31G*	141.8	137.2	139.5
	6-31 + G*	141.4	136.7	139.1
	6-31 + G**	142.1	137.4	139.7
TS1	6-311G*	139.2	134.5	135.9
	6-311 + G*	138.1	133.5	134.9
	6-311 + G**	140.8	136.2	137.8

that the improving basis sets from 6-31G* to 6-311 + G** has only insignificant effect to the calculated barrier height and exothermicity of the reaction. In addition to this, calculated kinetic parameters are smaller than the experimental values which is another certificate for the underestimation of the energy using the B3LYP method in the energy calculations [11,13–17]. A comparison of the calculated and experimental kinetic values demonstrates a nearly good agreement especially at the B3LYP/6-31 + G** level of the theory.

Energetics of the reactant, transition states, intermediate and products shows that the global pyrolysis process is spontaneous.

Free energy profile for the pyrolysis process of 2PAA is presented in Fig. 3. At first sight, it appears clearly that the second step of the concerted pathway is kinetically more favorable than the first step and hence, the first step is the rate determining step of the global process. Activation energy for the second step of only 67.5 kJ mol^{-1}.

To better analyze the extent of the bond breaking and bond formation through the reaction proceeding, the bond order concept has been applied [25,26]. The wiberg bond

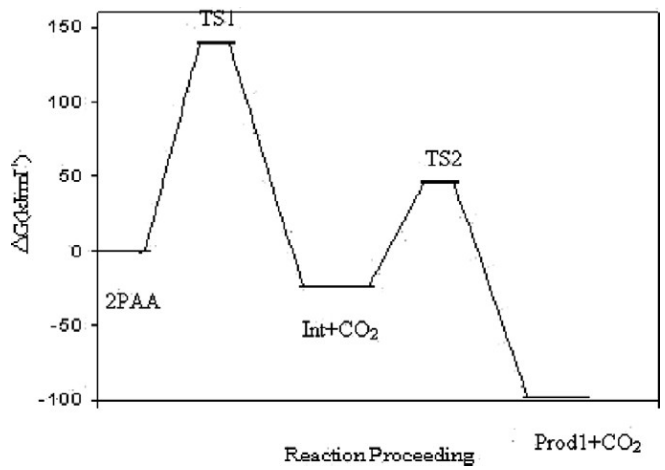

Fig. 3. Free energy profile evaluated at the B3LYP/6-31G* level for the pyrolysis reaction of 2PAA in the gas phase.

Table 12
Wiberg bond indices (Bi) and percentage of evolution through the chemical process (%Ev) of the bond indices at the TS1 calculated by means of the B3LYP/6-31G* level

	H1–N2	N2–C3	C3–C4	C4–C5	C5–O6	O6–H1
Bi^R	0.09	1.37	1.01	0.96	1.09	0.63
Bi^{TS}	0.48	1.24	1.21	0.65	1.34	0.25
% Ev	56.1	42.2	29.1	31.7	31.7	59.9
Sy			0.84			

indices have been calculated using the NBO analysis. The nature of the concerted mechanism has been monitored by means of the synchronicity (Sy) concept [27]. The results of these computations are reported in Table 12.

The percentages of evolution of the bond orders are within a range of 29–60%, describing a somewhat asynchronouse TS. The displacement of H1 atom is the most advanced motion, while the C3–C4 bond breaking and C5–O6 bond formation which include a single and double bond, respectively, are late displaying a small evolution percentage. The synchronicity value of 0.843 shows that the reaction pathway can be described as concerted and slightly asynchronous.

5. Conclusion

Kinetics and mechanism of 2-pyridylacetic acid pyrolysis was studied experimentally and theoretically in the gas phase and a valid reaction channel was established.

1. The pyrolysis reaction is homogeneous, unimolecular and obeys the first-order rate law.
2. Three probable mechanisms have been postulated, radical, zwitterionic and concerted mechanisms, and the concerted one is preferred to other pathways.
3. An analysis of the atomic charges suggests that the initial migration of H1 atom with the extension of C4–C5 bond can be regarded as driving force for the pyrolysis reaction.
4. Theoretical and experimental results are in good agreement, describing an asynchronous six-center concerted mechanism.

Acknowledgements

The authors thank J. Rezanejad (Management of the Gonabad University of Payam-e-Noor, Gonabad, Iran), Dr. A. Habibi (University of Ardabil, Iran) and M. Harati (University of Windsor, Canada) for helpful comments.

References

[1] V.S. Safont, V. Moliner, J. Anders, L.R. Domingo, J. Phys. Chem. 101 (1997) 1659.
[2] L.R. Domingo, J. Anders, V. Moliner, V.S. Safont, J. Am. Chem. Soc. 119 (1997) 6415.
[3] L.R. Domingo, M.T. Pitcher, J. Anders, V.S. Safont, G. Chuchani, Chem. Phys. Lett. 274 (1997) 422.

[4] L.R. Domingo, M.T. Pitcher, J. Anders, V.S. Safont, J. Anders, G. Chuchani, J. Phys. Chem. A 103 (1999) 3935.
[5] G. Chuchani, R.M. Dominguez, A. Herize, R. Romero, J. Phys. Org. Chem. 13 (2000) 757.
[6] C. Merrit Jr., D.H. Robertson, J. Gas Chromatogr. 5 (1967) 96.
[7] K. Kanomata, Y. Mashiko, J. Chem. Soc. Jpn. 87 (1967) 96.
[8] J. Vollman, P. Kriemler, I. Omura, J. Seidl, W. Simon, Microchem. J. 11 (1966) 7.
[9] Y. Ding, K.K. Jespersen, Chem. Phys. Lett. 199 (1992) 261.
[10] G.H. Coleman, H.F. John, Org. Syn. 8 (1976) 183.
[11] M.R. Gholami, M. Izadyar, J. Phys. Org. Chem. 16 (2003) 53.
[12] M.J. Frisch, G.W. Trucks, H.B. Schlegel, G.E. Scuseria, M.A. Robb, J.R. Cheeseman, V.G. Zakrzewski, J.A. Montgomery, R.E. Stratmann, J.C. Burant, S. Dapprich, J.M. Millam, A.D. Daniels, K.N. Kudin, M.C. Strain, O. Farkas, J. Tomasi, V. Barone, M. Cossi, R. Cammi, B. Mennucci, C. Pomelli, C. Adamo, S. Clifford, J. chterski, G.A. Petersson, P.Y. Ayala, Q. Morokuma, K. Cui, D.K. Malick, A.D. Rabuck, K. Raghavachari, J.B. Foresman, J. Ciolowski, J.V. Ortiz, B.B. Stefanov, G. Liu, A. Liashenko, P. Piskorz, I. Komaromi, R. Gomperts, J.L. Martin, D.J. Fox, T. Kieth, M.A. Al-Laham, C.Y. Peng, A. Nanayakkara, C. Gonzalez, M. Challacombe, P.M.W. Gills, B. Jonhson, W. Chen, M.W. Wong, J.L. Andres, M. Head-Gordon, E.S. Replogle, J.A. Pople, Gaussian 98 Revision A.9, Gaussian Inc, Pittsburgh PA, 1998.
[13] M. Izadyar, A.H. Jahangir, M.R. Gholami, J. Chem. Res. (2004) 585.
[14] M.R. Gholami, M. Izadyar, J. Mol. Struct. (THEOCHEM) 673 (2004) 61.
[15] M. Izadyar, M.R. Gholami, M. Haghgu, J. Mol. Struct. (THEOCHEM) 686 (2004) 37.
[16] M.R. Gholami, M. Izadyar, Chem. Phys. 301 (2004) 45.
[17] M.R. Gholami, M. Izadyar, in: Proceeding of the 6th Iranian Physical Chemistry Seminar, Urmia University, Iran, 2002, p. 31.
[18] T.J. Lee, C.W. Bauschlischer, C.E. Dateo, J.E. Rice, Chem. Phys. Lett. 228 (1984) 583.
[19] H.B. Schlegel, C. Peng, P.Y. Ayala, M.J. Frisch, J. Comput. Chem 17 (1996) 49.
[20] S. Glasstone, K.J. Laidler, H. Eyring, The Theory of Rate Processes, McGraw-Hill, New York, 1941.
[21] K.J. Laidler, Theories of Chemical Reaction Rates, McGraw-Hill, New York, 1941.
[22] A.E. Reed, L.A. Curtiss, F. Weinhold, Chem. Rev. 88 (1988) 899.
[23] A.E. Reed, R.B. Weinstock, F. Weinhold, J. Chem. Phys. 78 (1983) 4066.
[24] J. Lafont, A. Ensuncho, R.M. Dominguez, A. Rotinev, A. Herize, J. Quijano, G. Chuchani, J. Phys. Org. Chem. 16 (2003) 84.
[25] G. Lendvay, J. Mol. Struct. (THEOCHEM) 167 (1988) 331.
[26] G. Lendvay, J. Phys. Chem. 93 (1989) 4422.
[27] A. Moyano, M.A. Pricas, A. Valenti, J. Org. Chem. 54 (1989) 573.